A Harmonic Model for Loads Analysis and Control Design of a 2-bladed Wind Turbine

Daniel S. Zalkind* Lucy Y. Pao†
University of Colorado Boulder, Boulder, CO, 80309

I. Introduction

We will present a harmonic model of the interaction between different wind turbine component loads and an evaluation of a control algorithm that uses the model to reduce fatigue damage on the main bearing of a downwind, 2-bladed rotor. Wind turbines are large, dynamic structures, with components that experience large structural loads during extreme wind events and must survive fatigue load cycles over their twenty-year lifespan. Wind and gravity create loads on the blades, which transfer to the hub and onto the main bearing, yaw bearing and through the tower to the substructure. Each of these components experiences a different load profile as the wind speed varies, but due to the connection between the components, they are related. We will estimate load transfer functions to describe the relationship between different component loads. Using these load transfer functions, we will then control the structural loading on the wind turbine through blade pitch action.

Two-bladed wind turbines offer an interesting opportunity to reduce the tower-top blade mass and rotor cost by reducing overall material costs. However, the structural loading on the non-rotating parts of a two-bladed wind turbine is much larger than for three-bladed wind turbines. The moment of inertia of the rotor about the hub (in the non-rotating frame) changes with rotor position for two-bladed rotors, whereas it is constant and symmetrical for three-bladed rotors; this affects how loads are transferred from the rotating to the non-rotating turbine components. This dependence on rotor position lends itself well to a periodic analysis, which has been previously done, e.g., in [1] and [2]. In this paper, we will analyze each turbine component and their relationship to one another through their harmonic load components.

An unbalanced wind field, e.g., wind shear, causes the wind turbine components to experience an N-per-revolution (NP) load cycle as the rotor moves through the wind. Wind shear is the dominant dynamic in many instances, including turbulence, so we simulate wind turbines with a steady wind shear and compute the periodic load components on the wind turbine. These periodic components describe the magnitude and phase (and hence peak location) of the cyclic loading on the wind turbine part. Control of blade loads has been performed using these components in [3] and they are related to the multi-blade-coordinate transform [4] that is typically used for individual pitch control (IPC). In this study, we will focus on the relationship between component loads, e.g., how blade load harmonic components map to the hub load harmonics and analyze these relationships as the loads transfer from the blades to the tower base.

Through these relationships, control solutions can be designed to mitigate periodic loading on the different wind turbine components. In this paper, we will present the design of an individual pitch controller to reduce fatigue loads on the main bearing. Section II will present the model used to determine the harmonic components. In Section III, we will outline the relationship between the different wind turbine component loads. A control design for reducing main bearing loads will be presented in Section IV, and a summary of the on-going and future work is presented in Section V.

II. Harmonic Model for Wind Turbine Component Loads

We have developed a model for estimating wind turbine extreme and fatigue loads from aeroelastic simulations. Any wind turbine code could be used, but here we compute load signals from FAST [5]. With a wind turbine in sheared inflow, the wind speed u varies with height z

$$u(z) = u_h \left(\frac{z}{z_h} \right)^{\alpha}, \tag{1}$$

where z_h is the hub height, u_h is the hub-height wind speed, and $\alpha = 0.14$, which is representative of an offshore wind site. Due to wind shear, the predominant dynamics in the load signal are periodic, i.e., a load signal $m(\psi)$ can be expressed as

$$m(\psi) = m_0 + m_c^{1\mathrm{P}} \cos(\psi) + m_s^{1\mathrm{P}} \sin(\psi) + \ldots + m_c^{i\mathrm{P}} \cos(i\psi) + m_s^{i\mathrm{P}} \sin(i\psi) + \ldots \tag{2}$$

*Graduate Research Assistant, Electrical, Computer, and Energy Engineering.
†Professor, Electrical, Computer, and Energy Engineering.

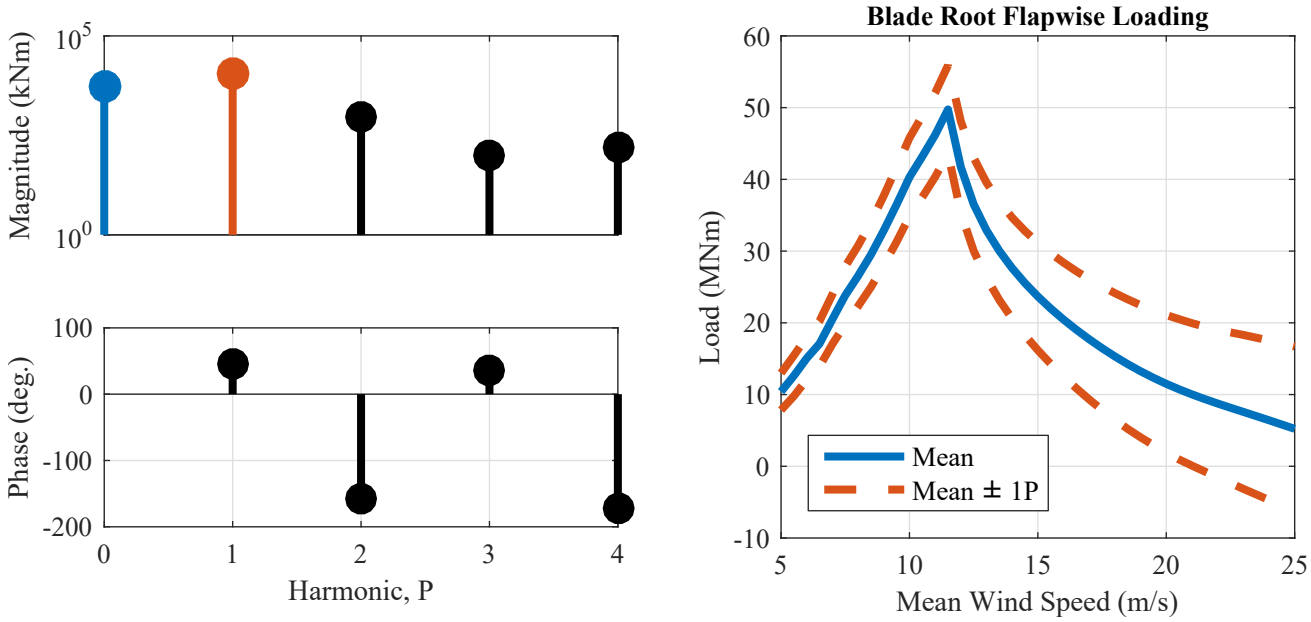

Fig. 1 The load harmonic magnitude $|m^{i\mathrm{P}}|$ and phase $\phi^{i\mathrm{P}}$ for the 0th through 4th periodic harmonic of the blade root load in the flapwise direction (left). The mean load (right, blue) is superimposed with the 1P harmonic amplitude (right, red) across wind speeds.

where ψ is the azimuthal position of the rotor. The harmonic components are computed by

$$m_0 = \frac{1}{2\pi N_R}\int_{\psi-2\pi N_R}^{\psi} m(\psi)d\psi, \tag{3}$$

$$m_c^{i\mathrm{P}} = \frac{1}{2\pi N_R}\int_{\psi-2\pi N_R}^{\psi} m(\psi)\cos(i\psi)d\psi, \tag{4}$$

and

$$m_s^{i\mathrm{P}} = \frac{1}{2\pi N_R}\int_{\psi-2\pi N_R}^{\psi} m(\psi)\sin(i\psi)d\psi, \tag{5}$$

where N_R is the number of rotations used in the calculation. Load signals can be reconstructed closely using the first four harmonics; most of the energy is usually in either the 1st or 2nd harmonic for two-bladed turbines, depending on whether the component is rotating (1P) or non-rotating (2P).

From the components in (4) and (5), the periodic components of a load signal $m^{i\mathrm{P}}$ can be expressed in terms of a complex number, with a magnitude and phase,

$$|m^{i\mathrm{P}}| = \sqrt{(m_c^{i\mathrm{P}})^2 + (m_s^{i\mathrm{P}})^2}, \tag{6}$$

and

$$\angle m^{i\mathrm{P}} = \tan^{-1}\left(\frac{m_s^{i\mathrm{P}}}{m_c^{i\mathrm{P}}}\right), \tag{7}$$

respectively, which describes how the periodic signal varies with the rotor azimuth ψ. Note that the 0P load component is strictly real. An example for the blade flapwise load is shown in Fig. 1. We can use these harmonic coefficients to estimate peak and fatigue loads, as well as describe the wind turbine loading as they transfer through the structure.

A. Turbine Model Description

In this paper, we analyze the loads of a downwind, 2-bladed, large rotor concept, called the Segmented Ultralight Morphing Rotor (SUMR); it is summarized in Table 1. The concept is first described in [6] and the aerodynamic design

Table 1 SUMR Turbine Description Summary

Turbine Parameter	Value
Rated Power	13.2 MW
Rated Rotor Speed	9.90 rpm
Hub Height	142.4 m
Rotor Radius	106.8 m
Rotor Position	Downwind
Blade Mass	54.8 Mg
Number of Blades	2
Max Chord	7.22 m
Cone Angle	12.5 deg.

of the rotor we simulate is presented in [7]. The structural layup [8] is designed so that the blade mass is reduced by 25% from a 13.2 MW 3-bladed conventional rotor [9]. The rotor has been structurally validated, checking for strain limits, panel buckling, and fatigue with a closed-loop controller for the power-producing Design Load Cases [10]

III. Load Transfer Functions

Loads on different wind turbine parts can be related by their harmonic components. We refer to these relationships as load transfer functions and describe their estimation using simulation data in this section.

A. Description of Load Axes and Method for Estimating Transfer Function

The load axes are shown in Fig 2. Structural loads originate from the aerodynamic interaction of the blades with the wind and from the weight of the structure itself. Blade root loads (b) transfer to the rotating hub (h) at the pitch bearing. The hub is connected to the main shaft, which is supported by the main bearing (m). The main bearing is bolted to the nacelle bedplate and connected to the yaw bearing (y). Loads from the rotor-nacelle assembly transfer down the tower to the base (t), which is connected to the wind turbine substructure. The blade and hub loads are computed in the rotating frame, while the main bearing, yaw bearing, and tower base loads are computed in the non-rotating frame.

Given two load signals, $m_1, m_2 \in \mathbb{C}$, this representation can be used to describe the magnitude and phase of the load as it varies with ψ. A linear load transfer function represents the linear mapping from m_1 to m_2, i.e.,

$$m_2 = a^* \begin{bmatrix} m_1 \\ 1 \end{bmatrix} \tag{8}$$

where $a \in \mathbb{C}^2$ and $(^*)$ denotes the complex conjugate transpose. Using multiple wind speeds u_i, the linear coefficients a can be estimated in a linear least squares sense using $N \geq 2$ wind speed samples

$$\begin{bmatrix} m_2^*(u_1) \\ m_2^*(u_2) \\ \vdots \\ m_2^*(u_N) \end{bmatrix} = \begin{bmatrix} m_1^*(u_1) & 1 \\ m_1^*(u_2) & 1 \\ \vdots & \vdots \\ m_1^*(u_N) & 1 \end{bmatrix} a, \tag{9}$$

which can be represented in block matrix form as

$$M_2 = M_1 a. \tag{10}$$

Finally, the linear coefficients a can be estimated in a least squares sense by

$$\hat{a} = (M_1^* M_1)^{-1} M_1^* M_2. \tag{11}$$

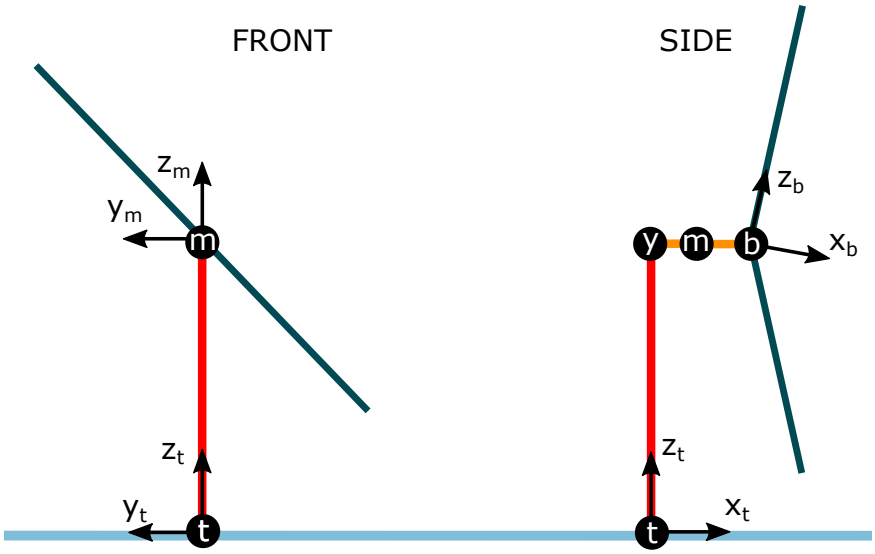

Fig. 2 Illustration of the load axes used in this paper. The non-rotating loads (tower, main bearing, and yaw bearing) are all parallel (and are denoted by subscripts t, m, and y, respectively). Blade and hub load axes rotate with azimuth angle.

In pitch regulated turbines, like the one we are adressing, there is a distinct difference in the load signals in below rated (Region II) and above rated (Region III) control. Once collective pitch control is used to regulate the wind speed in Region III, the thrust loads on the rotor are greatly reduced. Because of this discrete change in load signals, we will separately account for Region II and Region III load signals where appropriate.

B. Blade to Hub

The hub loads are a combination of the blade loads. Considering the symmetry of the blades and wind inflow, we only use load signals $m_{by,1}$, for one blade to estimate the hub loads m_{hy} and m_{hz}, namely

$$\begin{bmatrix} m_{hy} \\ m_{hz} \end{bmatrix} = \begin{bmatrix} a^*_{hy,b} \\ a^*_{hz,b} \end{bmatrix} \begin{bmatrix} m_{by,1} \\ 1 \end{bmatrix}. \tag{12}$$

The magnitude of each hub load versus the blade y-direction load is shown in Fig. 3 and demonstrates that a relationship exists. Fig. 3 (left) shows that there is a linear relationship between the y-direction blade loads and the y-direction hub loads, but that it is different for Region II and Region III operation. Future work will explore this difference in more detail, with the goal of developing a combined model that incorporates the effect of the collective blade pitch into a single load transfer function.

The right side of Fig. 3 shows that the z-direction hub load magnitudes are almost independent of the y-direction blade loads. The hub z-direction load is primarily dependent on the rotor center of mass for 2-bladed rotors.

C. Hub to Main Bearing

The rotating hub and main shaft are supported by the non-rotating main bearing, which is typically a small distance from the hub. For simplicity, we model the loads at the hub and main bearing at the same location. To estimate the main bearing loads, a rotation transformation is applied to the hub loads to estimate the main bearing loads:

$$\begin{bmatrix} m_{my} \\ m_{mz} \end{bmatrix} \begin{bmatrix} \cos(\psi) & -\sin(\psi) \\ \sin(\psi) & \cos(\psi) \end{bmatrix} \begin{bmatrix} m_{hy} \\ m_{hz} \end{bmatrix}. \tag{13}$$

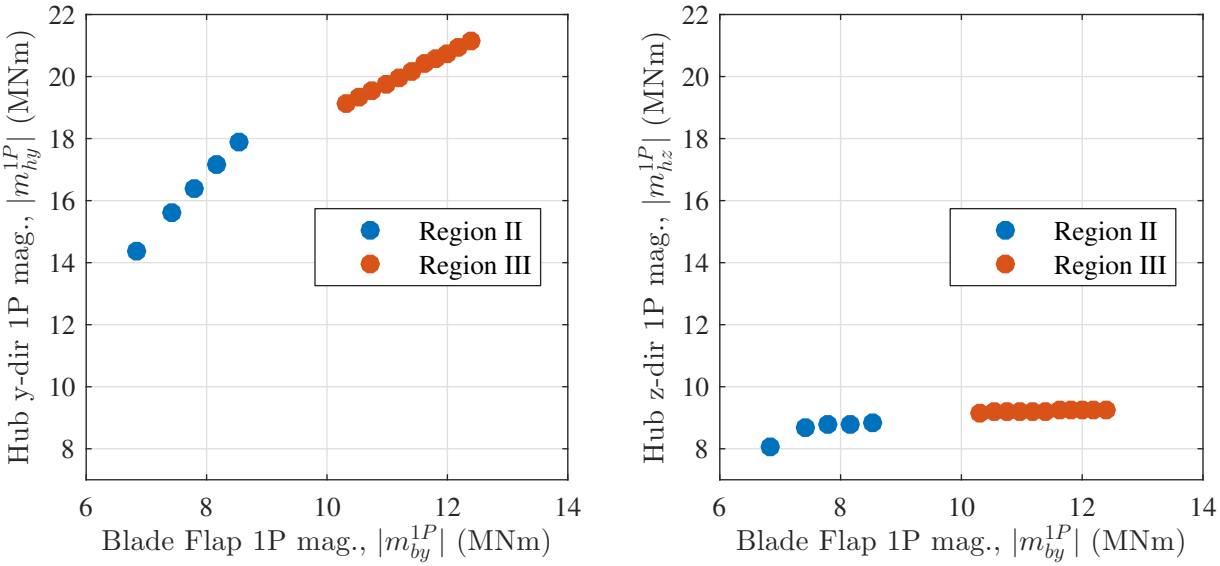

Fig. 3 Relationship between blade flap 1P magnitude and shaft loads in the y- and z-directions.

In terms of the dominant periodic load signals,

$$m_{my}^{0P} = \frac{1}{2}\mathrm{Re}\{m_{hy}^{1P} + jm_{hz}^{1P}\}, \tag{14}$$

$$m_{my}^{2P} = \frac{1}{2}(m_{hy}^{1P} - jm_{hz}^{1P}), \tag{15}$$

$$m_{mz}^{0P} = \frac{1}{2}\mathrm{Re}\{m_{hz}^{1P} + jm_{hy}^{1P}\}, \text{ and} \tag{16}$$

$$m_{mz}^{2P} = \frac{1}{2}(m_{hz}^{1P} + jm_{hy}^{1P}). \tag{17}$$

For the SUMR rotor, we have compared the main bearing loads estimated from (14)-(17) and the actual load values from simulation. The results are shown in Fig. 4. The one-to-one relation across wind speeds, for both the real and imaginary components, indicates that the model presented is in good agreement with the computed loads.

D. Main Bearing to Yaw Bearing and Tower Base

We model the non-rotating load components (main bearing, yaw bearing, and tower base) using a linear transfer function. Fig. 5 demonstrates the load transfer function from the main bearing to the yaw bearing. The 0P mean loads in the y-direction (upper, left) requires a different mapping for Region II and Region III due to the effect of pitch control on the yaw bearing. The 0P load transfer function in the z-direction (lower, left), however, is nearly constant across operating regions. The 2P cyclic loads in both directions (right) demonstrate good agreement across operating regions for both the real and imaginary parts.

The mapping from the yaw bearing to the tower base loads is depicted in Fig. 6, and we observe several issues. The 0P load component (left) in Region III is clearly not dependent on the yaw bearing. Since Region III pitch control drastically changes the thrust on the rotor, which is the primary driver of loads on the tower base, perhaps the yaw bearing is not the correct map to the tower base in this operating region. Future work will investigate the effect of the collective pitch command and blade load on the tower base load. For the 2P cyclic loading on the tower base, the relationship is non-linear in Region II. In Region II, there is a resonance in the tower motion when the 2P rotor frequency is near the tower natural frequency, which is responsible for the non-linearity. The resonance is primarily in the side-to-side direction, which is not depicted here, but we will further analyze and develop another controller and present these results in the final paper.

IV. Control Using Harmonic Components

Using the relationships derived in the previous section, we can derive controllers that influence the harmonic components of the wind turbine. Individual blade pitch control (IPC) can be used to change the loading on the blades,

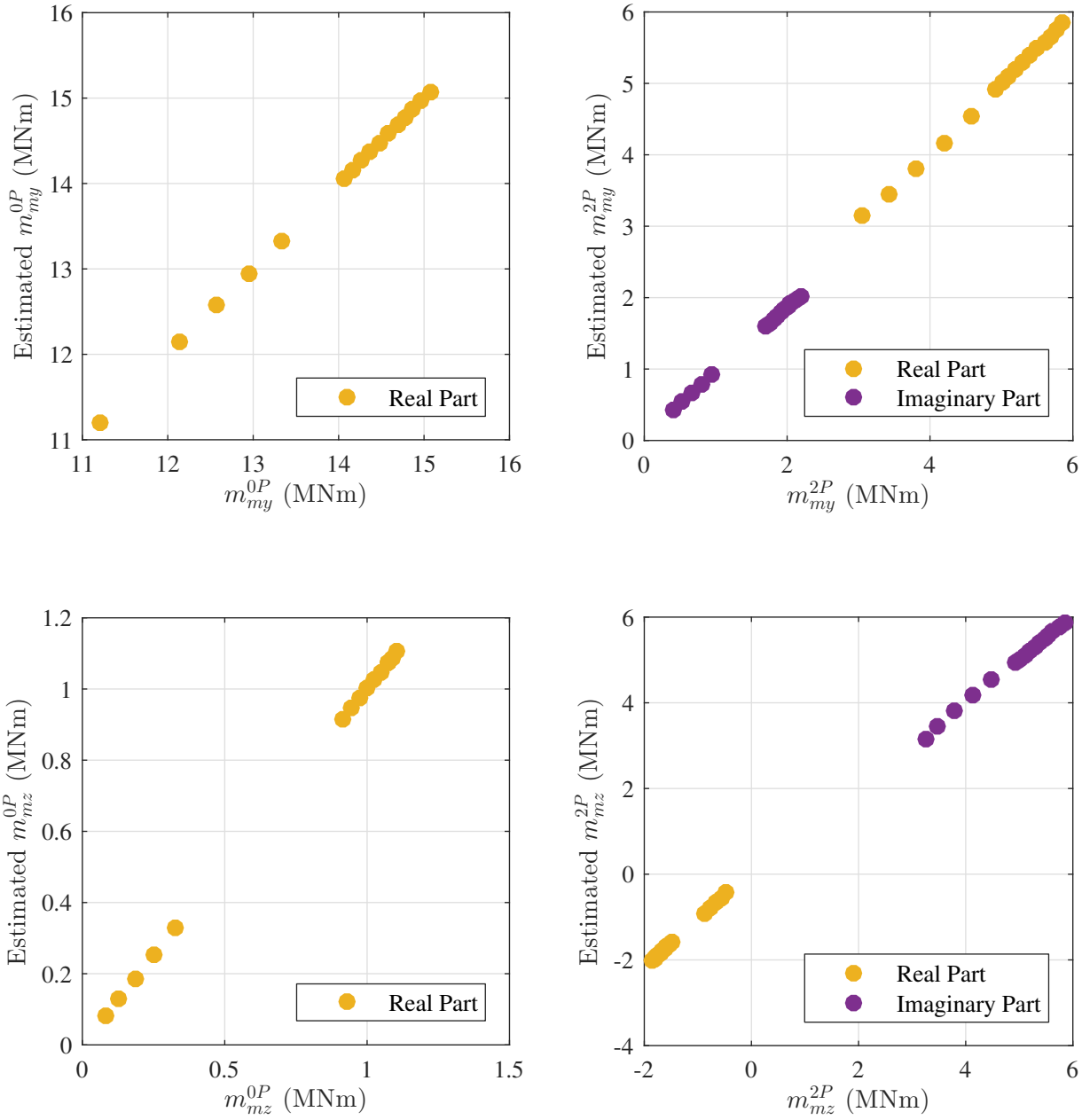

Fig. 4 Main bearing loads computed from simulation (x-axis) and main bearing loads estimated from hub loads in (14)-(17)**.**

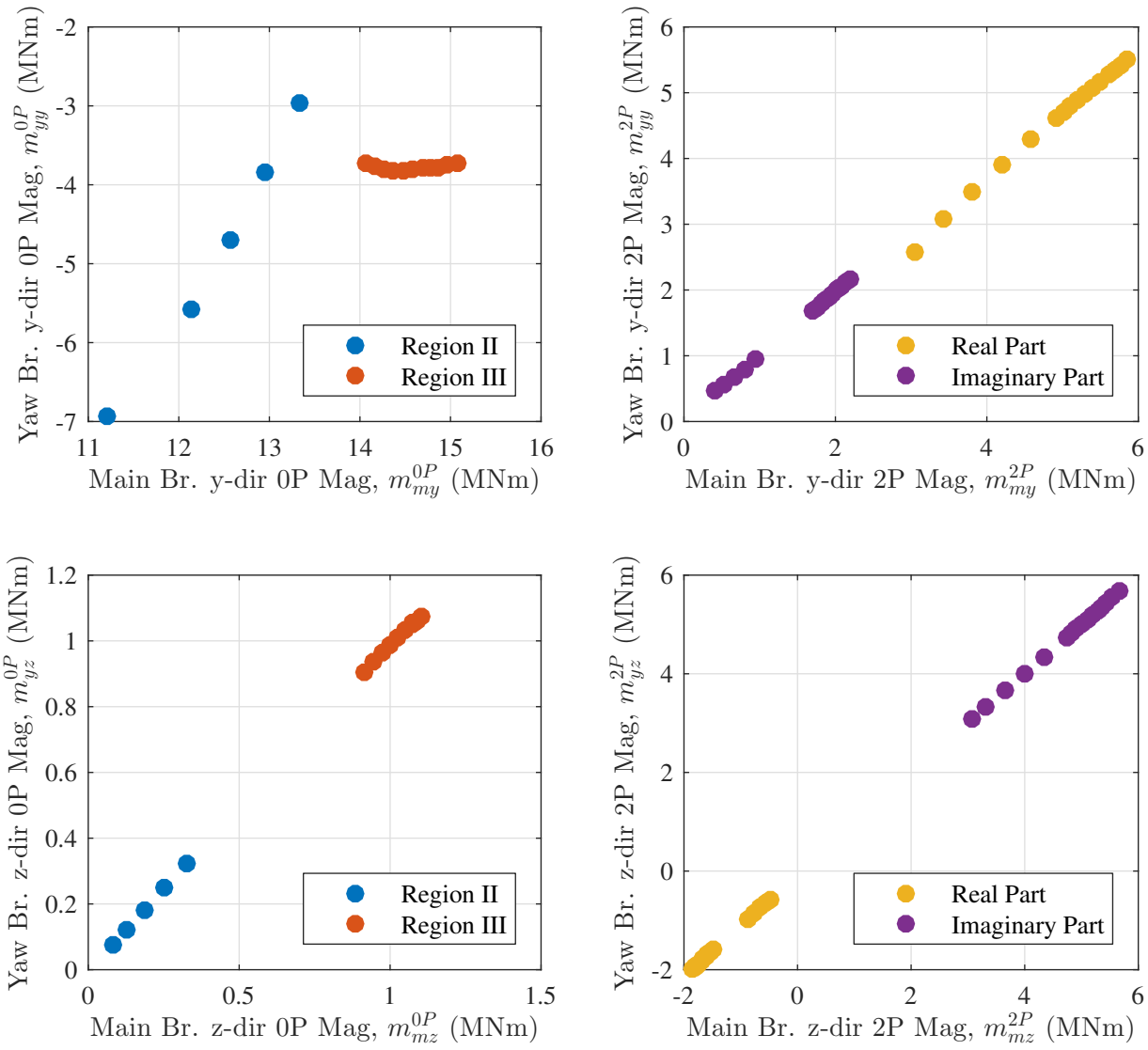

Fig. 5 Relationship between the main bearing (m) and the yaw bearing (y) in the y-direction (top) and z-direction (bottom) for the 0P load component (left) and the 2P load component (right). Both the real and imaginary parts are shown for the 2P load component.

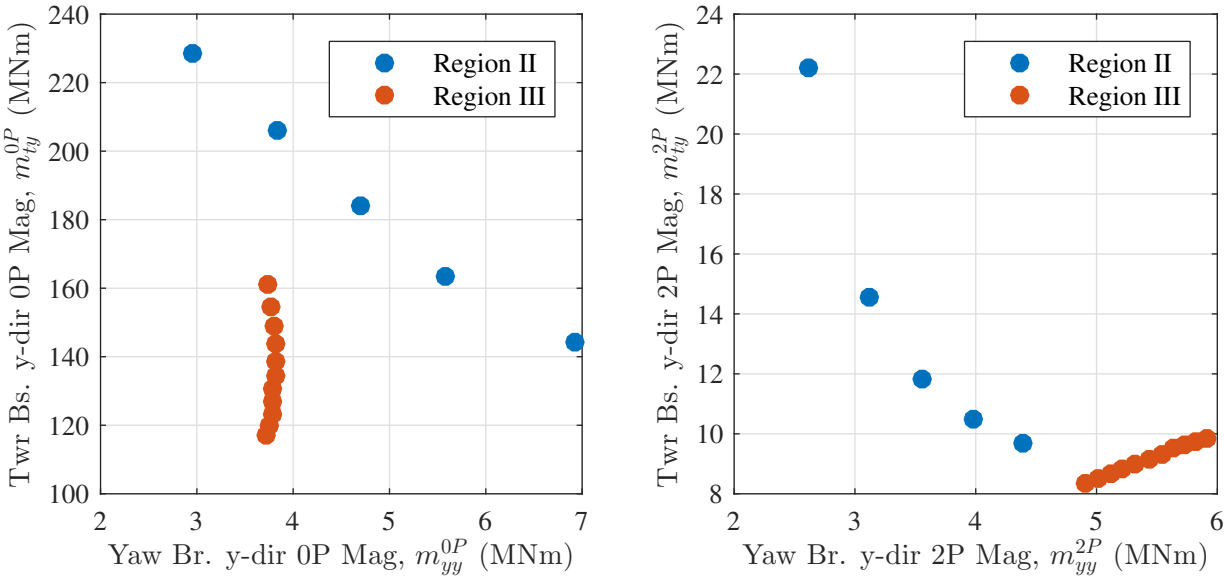

Fig. 6 Relationship between the yaw bearing (y, horizontal axis) and the tower base (t, vertical axis) in the y-direction for the 0P (left) and 2P harmonic (right) load components for Region II and Region III control.

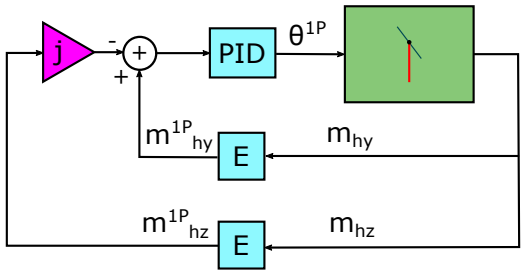

Fig. 7 Proof-of-concept control block diagram to enforce the relationship in (20) **though individual pitch control θ^{1P}. The load harmonics are estimated (E) using** (4) **and** (5)**.**

which alters the harmonic loading on the hub. In this paper, we present an individual pitch controller designed to reduce the 2P loading on the main bearing. A 1P IPC input ($\theta^{1P} \in \mathbb{C}$) can control the y-direction hub load m_{hy}^{1P}. The IPC input θ^{1P} is converted into

$$\theta_1 = |\theta^{1P}| \cos(\psi + \angle\theta^{1P}), \text{ and} \tag{18}$$

$$\theta_2 = |\theta^{1P}| \cos(\psi + \angle\theta^{1P} + 180^\circ) = -\theta_1, \tag{19}$$

where θ_1 and θ_2 are the real-valued pitch commands for blades 1 and 2, respectively. If our goal is to minimize the 2P main bearing loads m_{hy}^{2P} and m_{hz}^{2P}, from (15) and (17), we can see that the hub load must be controlled so that

$$m_{hy} = j m_{hz}. \tag{20}$$

To demonstrate the concept, we have designed a proportional-integral-derivative (PID) control loop (Fig. 7) that uses θ^{1P}, both magnitude and phase, to enforce (20). The harmonic components are estimated using (4),(5), and $N_R = 2$. A summary of the results from a steady wind simulation at 15 m/s is shown in Fig. 8.

We see that the hub y-direction magnitude and phase converge so that they are equal in magnitude and 90 degrees out of phase with the m_{hz}^{1P} harmonic component (left) using the IPC input (center). The 2P load magnitudes of the main bearing (right) are minimized once the set point is reached. Using this IPC controller reduces the main bearing 2P load drastically in steady state.

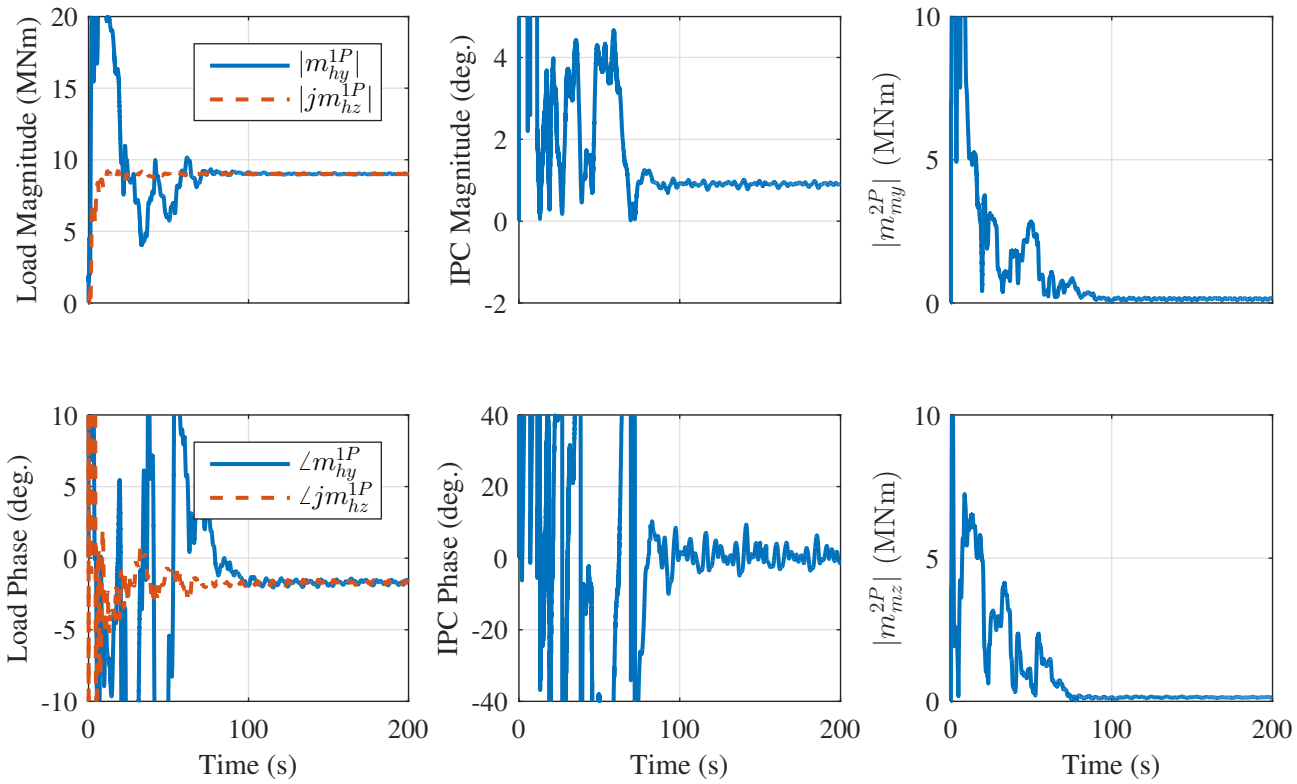

Fig. 8 Hub load magnitude and phase for the output and reference in (20)**, IPC magnitude and phase, and main bearing y-direction and z-direction 2P harmonic magnitude for a 15 m/s steady state example.**

To test the performance in a realistic environment, DLC 1.2 (normal turbulence model) simulations were performed, with less optimistic results. Compared to the baseline control, with no IPC, the IPC design presented here reduces the main bearing damage equivalent loads by about 15%. Future work will further refine the estimation and control techniques used to more quickly control and estimate harmonic components in a changing wind environment.

V. Conclusions and Future Efforts

We have presented the framework for a harmonic load model that can be used to analyze 2-bladed rotors and derive control laws. On-going work will focus on expanding and refining the load transfer functions, including tower side-to-side motion and control. Load transfer functions were presented in a uni-directional manner, meaning that loads from the blades transfer in one direction to the tower base. During tower resonance, it is clear that the tower motion impacts the loading on the other components. Therefore, a bi-directional load transfer model will also be explored. As previously stated, we will also incorporate the effect of collective pitch action into the load transfer function in order to unify the Region II and Region III mappings. The presented IPC control architecture will also be refined to improve performance in a non-steady wind environment.

Acknowledgments

The information, data, or work presented herein was funded in part by the Advanced Research Projects Agency - Energy (ARPA-E), U.S. Department of Energy, under Award Number DE-AR0000667. The views and opinions of authors expressed herein do not necessarily state or reflect those of the United States Government or any agency thereof.

References

[1] Stol, K., Balas, M., and Bir, G., "Floquet Modal Analysis of a Teetered-Rotor Wind Turbine," *Journal of Solar Energy Engineering*, Vol. 124, No. 4, 2002, p. 364. doi:10.1115/1.1504846.

[2] Hansen, M. H., "Modal dynamics of structures with bladed isotropic rotors and its complexity for 2-bladed rotors," *Wind Energy Science*, 2016, pp. 1–37. doi:10.5194/wes-2016-27.

[3] Bottasso, C. L., Croce, A., Riboldi, C. E., and Nam, Y., "Multi-layer Control Architecture for the Reduction of Deterministic and Non-deterministic Loads on Wind Turbines," *Renewable Energy*, Vol. 51, 2013, pp. 159–169. doi:10.1016/j.renene.2012.08.079.

[4] Bir, G., "Multiblade Coordinate Transformation and Its Application to Wind Turbine Analysis," *ASME Wind Energy Symposium*, 2008.

[5] Jonkman, J. M., and Marshall, B. L., "FAST User's Guide," Tech. rep., NREL, 2005.

[6] Ichter, B., Steele, A., Loth, E., Moriarty, P., and Selig, M., "A morphing downwind-aligned rotor concept based on a 13-MW wind turbine," *Wind Energy*, Vol. 19, No. 4, 2016, pp. 625–637. doi:10.1002/we.1855, URL `http://dx.doi.org/10.1002/we.1855`.

[7] Ananda, G. K., Bansal, S., and Selig, M. S., "Aerodynamic Design of the 13.2 MW SUMR-13i Wind Turbine Rotor," *ASME Wind Energy Symposium*, 2018. doi:10.2514/6.2018-0994.

[8] Paquette, J., "Structural Design of the SUMR-13 Wind Turbine Blade," Tech. rep., Sandia National Laboratories, 2017.

[9] Griffith, D. T., and Richards, P. W., "The SNL100-03 Blade : Design Studies with Flatback Airfoils for the Sandia 100-meter Blade," Tech. Rep. September, Sandia Report, 2014.

[10] International Electrotechnical Commission, "IEC 61400-1: Wind Turbines - Part 1: Design Requirements," Tech. rep., 2005.